Lecture 13: Stretching–folding–re-injection dynamics in cobweb diagrams, basin of attraction (maps), sensitive dependence on initial conditions (maps), linearisation of 2-D maps, classification of fixed points in 2-D maps, linear analysis of the Hénon map, video feedback effect

Contents

Handout: Classification of fixed points in 2-D linear maps.

1 Iterate dynamics of unimodal maps

1.1 Stretching–folding–re-injection dynamics and cobweb diagrams

We know that cobweb diagrams may and do represent chaotic dynamics via the cascade of period doubling bifurcations visible on orbit diagrams. The mechanism behind a chaotic solution should also includes the repeated stretching–folding–re-injection process first introduced in Lecture 11 and expanded upon in Lecture 12. Can we see it in cobweb diagrams? Let's consider a familiar unimodal map—the logistic map.

SLIDES: 3–5

Mixing-folding dynamics in cobweb diagrams

We consider the logistic map

$$x_{n+1} = r x_n (1 - x_n), \tag{1}$$

where r is the control parameter.

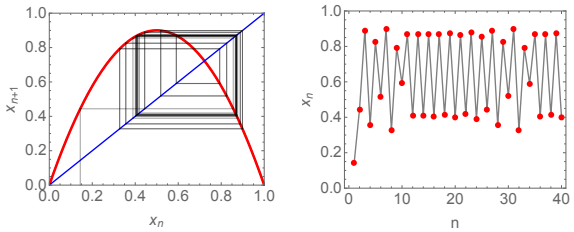

Can we see the stretching–folding–re-injection dynamics in chaotic cobweb plots?

D. Kartofelev YFX1520 3 / 24

Mixing-folding dynamics in cobweb diagrams

Dynamics of the interval $x_0 = [x', x'']$.

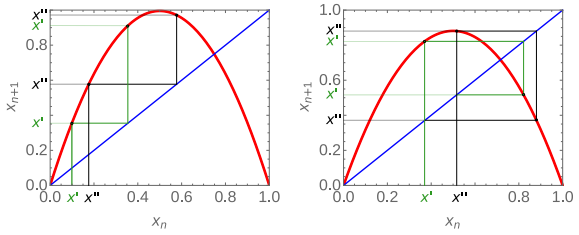

Stretching and squeezing of x_0. Mixing and folding of x_0.

D. Kartofelev YFX1520 4 / 24

Mixing-folding dynamics in cobweb diagrams

Dynamics of selected points $\{\alpha, \beta, \gamma, \delta\} \in x_0$.

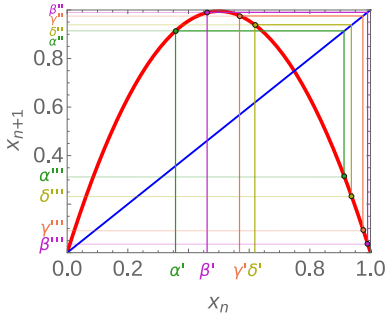

$$\{\alpha', \beta', \gamma', \delta'\} \xrightarrow[\text{mixing}]{} \{\alpha'', \delta'', \gamma'', \beta''\} \xrightarrow[\text{folding}]{} \{\beta''', \gamma''', \delta''', \alpha'''\}$$

D. Kartofelev YFX1520 5 / 24

So far we didn't think of the map function, shown with the red graph, in the manner shown above. But indeed, the interval $[0, 1]$ (the horizontal axis) is being mapped via **stretching and folding** it into the parabolic shape—a straight line $\rightarrow$ a parabola. The **re-injection step** is introduced by further map iteration steps.

1.2 Sensitive dependence on initial conditions

In addition to the stretching–folding–re-injection dynamics maps also feature a sensitive dependence on initial conditions (SDIC) that was present in the **chaotic** continuous-time models (ODEs) studied in our previous lectures. Below, we give a formal definition of the SDIC in maps. It can be shown that there are regions in map parameter space where this definition/criteria holds and where it does not hold. We remind that SDIC is central to chaotic dynamics in continuous-time systems.

Definition: Let $\vec{f}$ be a map on $\mathbb{R}^D$ where D is the map dimension. A point $\vec{x}_0$ has SDIC if exists $|\vec{d}| > 0$ such that any neighbourhood of $\vec{x}_0$ contains a point $\vec{x}$ where

$$\boxed{\left|\vec{f}^n(\vec{x}) - \vec{f}^n(\vec{x}_0)\right| \geq |\vec{d}|,} \tag{1}$$

where n denotes the map iterate so that f^n is the n-th iterate map, $\vec{d} = \vec{x} - \vec{x}_0$, and $|\vec{d}| \ll 1$.

SLIDES: 6–8

Sensitive dependence on initial conditions[1]

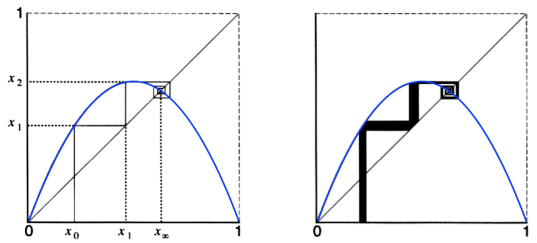

Figure: The logistic map where $1 < r < 3$. (Left) Iteration of a single point. (Right) Iteration of an interval. **No sensitivity** on initial condition for stable fixed point or period-p points.

[1]H. Peitgen, H. Jürgens, D. Saupe, *Chaos and Fractals: New Frontiers of Science*, New York: Springer-Verlag, 2004 pp. 471–473

D. Kartofelev YFX1520 6 / 24

Sensitive dependence on initial conditions[2]

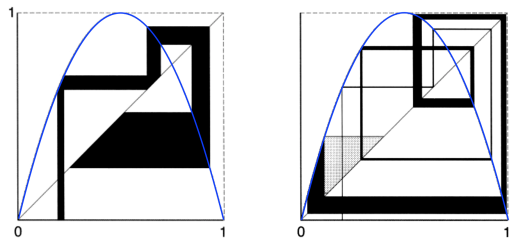

Figure: The logistic map where $r = 4$. (Left) Iteration of an interval of initial conditions. (Right) Iteration of an even smaller interval, also leading to large deviations.

[2]H. Peitgen, H. Jürgens, D. Saupe, *Chaos and Fractals: New Frontiers of Science*, New York: Springer-Verlag, 2004 pp. 471–473

D. Kartofelev YFX1520 7 / 24

Sensitive dependence on initial conditions[3]

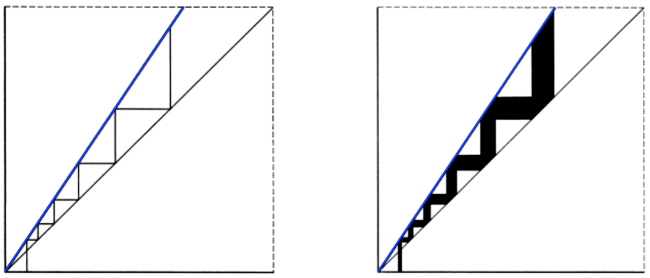

Figure: Map given by $x_{n+1} = cx_n$ where the constant $c > 1$. (Left) A single initial condition. (Right) An interval of initial conditions. The property of sensitivity to initial conditions **is central to chaos**. **Sensitivity, however, does not automatically lead to chaos in maps.**

[3]H. Peitgen, H. Jürgens, D. Saupe, *Chaos and Fractals: New Frontiers of Science*, New York: Springer-Verlag, 2004 pp. 471–473

D. Kartofelev YFX1520 8 / 24

A visual inspection of the evolution of the initial intervals demonstrates SDIC defined by (1). **The SDIC in maps does not automatically lead to chaos, i.e., chaotic dynamics.** Slide 8 shows how a non-chaotic linear map features SDIC.

1.3 Basin of attraction

Next, we define the basin of attraction in maps.

Definition: Let $\vec{f}$ be a map on $\mathbb{R}^D$ where D is the map dimension and let $\vec{x}^*$ be a stable fixed point or period-p point. The basin of attraction of $\vec{x}^*$ is the set of points $\vec{x}$ such that

$$\boxed{\lim_{n\to\infty}\left|\vec{f}^n(\vec{x}) - \vec{f}^n(\vec{x}^*)\right| = 0,} \tag{2}$$

where n denotes the iterate of map $\vec{f}$ where f^n is the n-th iterate map.

Let's consider the following example:

SLIDE: 9

Basin of attraction and a 2-D map

Example[4]: Determine the basin of attraction of the following nonlinear 2-D map given in polar coordinates

$$\begin{aligned} r_{n+1} &= r_n^2, \\ \theta_{n+1} &= \theta_n - \sin\theta_n. \end{aligned} \tag{2}$$

[4]See Mathematica .nb file uploaded to the course webpage.

D. Kartofelev YFX1520 9 / 24

The two-dimensional map given in polar coordinates is decoupled in r and θ. We can study the map's discrete dynamics in r and θ directions separately.

The following numerical file shows the dynamics of the map presented on Slide 9.

NUMERICS: NB#1

Dynamic animation of the iterates of a 2-D map given in the following form:

$$\begin{aligned} r_{n+1} &= r_n^2, \\ \theta_{n+1} &= \theta_n - \sin\theta_n, \end{aligned} \tag{3}$$

where r is the distance in the radial direction and θ is the angular displacement; The notion of a basin of attraction.

Figure 1 shows the cobweb diagrams of the individual one-dimensional decoupled maps that form the two-dimensional map (3) that is also shown on Slide 9.

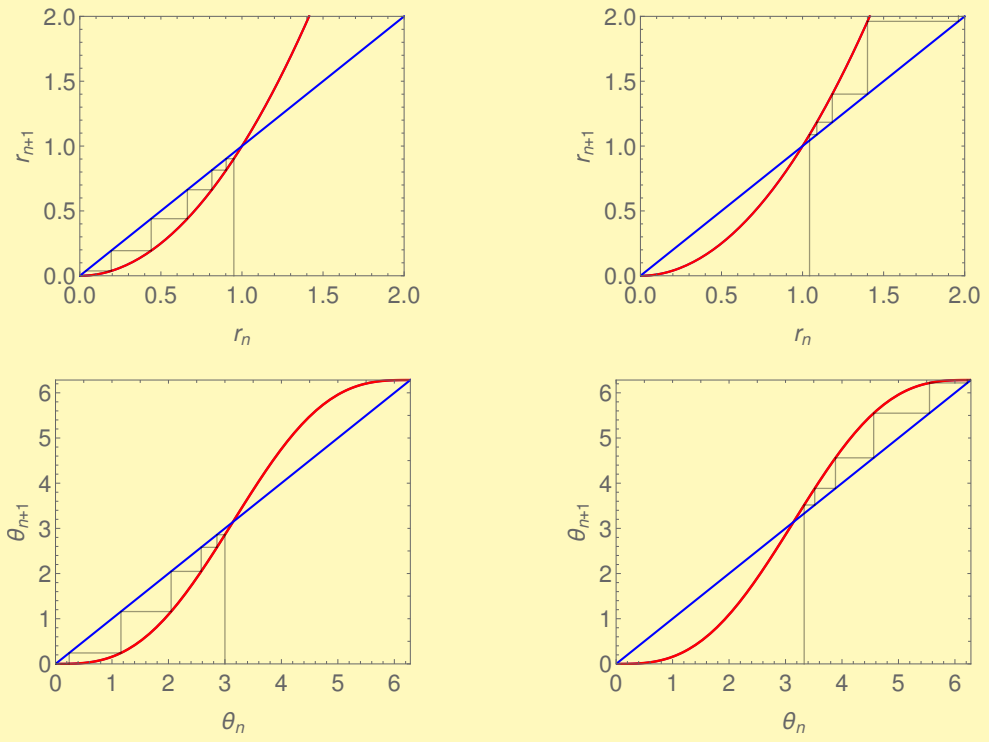

Figure 1: (Top row) Map dynamics in the radial direction shown for initial condition $r_0 \lesssim 1$ and $r_0 \gtrsim 1$. (Bottom row) Map dynamics in terms of the angular displacement for initial angle $\theta_0 \lesssim \pi$ and $\theta_0 \gtrsim \pi$.

The analysis of the decoupled one-dimensional maps that form the full two-dimensional map leads us to conclude that the overall dynamics must be as shown in Fig. 2. The basin of attraction defined by (2) is the set of points inside the open unit circle $r < 1$, $0 \leq \theta < 2\pi$. The phase portrait trajectories shown with the continuous curves in Fig. 2 are discretely sampled by map iterates (r_n, θ_n). The iterates *hop* along these trajectories. This observation and possible exceptions to it are further expanded upon and explained in Secs 1.4 and 3.4.

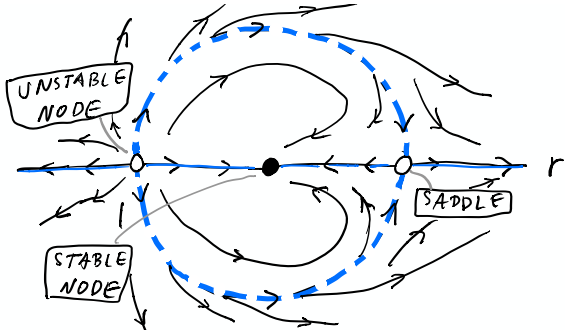

Figure 2: Phase portrait of the map (3) that is also defined on Slide 9. The basin of attraction defined by the open unit circle $r < 1$ and $0 \leq \theta < 2\pi$. Manifold that separated the **stable and unstable basins of attraction** is the unit circle shown with the blue dashed curve. The iterates of an initial condition *hop* along the continuous phase portrait *trajectories*. Four invariant sets present in the phase portrait (on the horizontal) are indicated by blue continuous lines.

Numerical simulation of the map confirms the aforementioned conclusions.

NUMERICS: NB#1

Dynamic animation of the iterates of a 2-D map given in the following form:

$$\begin{aligned} r_{n+1} &= r_n^2, \\ \theta_{n+1} &= \theta_n - \sin\theta_n, \end{aligned} \tag{4}$$

where r is the distance in the radial direction and θ is the angular displacement; The notion of a basin of attraction.

1.4 General solution and phase portrait of linear 2-D map

The general form of an iterated map is

$$\vec{x}_{n+1} = \vec{f}(\vec{x}_n), \tag{5}$$

where $\vec{f}$ is the given map function on $\mathbb{R}^D$ and where D is the map dimension, $\vec{x}_n$ is the iterated map value for n-th iterate. Function $\vec{f}$ can be either linear or nonlinear.

Let's revisit the calculation of iterates $\vec{x}_n$ of a linear two-dimensional map (5) where $D = 2$ and $\vec{x}_n = (x_n, y_n)^T$. The component form of the map is the following:

$$\begin{cases} x_{n+1} = ax_n + by_n, \\ y_{n+1} = cx_n + dy_n. \end{cases} \tag{6}$$

The corresponding matrix form is

$$\vec{x}_{n+1} = A\vec{x}_n, \tag{7}$$

where the system coefficient matrix

$$A = \begin{pmatrix} a & b \\ c & d \end{pmatrix}, \tag{8}$$

and it has real valued coefficients, $\{a, b, c, d\} \in \mathbb{R}$.

Thus, the iterates $\vec{x}_n$ of linear map may be calculated as follows

$$\begin{aligned}
\vec{x}_1 &= A\vec{x}_0, \\
\vec{x}_2 &= A\vec{x}_1 = A \cdot A\vec{x}_0 = A^2\vec{x}_0, \\
\vec{x}_3 &= A\vec{x}_2 = A \cdot A^2\vec{x}_0 = A^3\vec{x}_0, \\
&\vdots \\
\vec{x}_n &= A\vec{x}_{n-1} = A^n\vec{x}_0,
\end{aligned} \tag{9}$$

where A^n denotes the matrix raised to the n-th power. This practically useful result is valid for linear maps only. It can be shown that the two-dimensional component form of iterates (9) in terms of their map eigenvalues and eigenvectors, i.e., the general solution of the map has the form

$$\begin{cases} x_n = C_1\lambda_1^n\vec{v}_1, \\ y_n = C_2\lambda_2^n\vec{v}_2, \end{cases} \tag{10}$$

where n is the map iterate, λ_1 and λ_2 are the eigenvalues, $\vec{v}_1$ and $\vec{v}_2$ are the eigenvectors, and C_1 and C_2 are the constants that are resolved from an initial condition $\vec{x}_0 = (x_0, y_0)^T$. For comparison the general solution to a linear ODE defined by

$$\dot{\vec{x}} = B\vec{x}, \tag{11}$$

where $\vec{x} = (x, y)^T$ and B is the system coefficient matrix, is in the form

$$\begin{cases} x(t) = C_1\mathrm{e}^{\lambda_1 t}\vec{v}_1, \\ y(t) = C_2\mathrm{e}^{\lambda_2 t}\vec{v}_2, \end{cases} \tag{12}$$

where t is the time, λ_1 and λ_2 are the eigenvalues, $\vec{v}_1$ and $\vec{v}_2$ are the eigenvectors of the system matrix B, and C_1 and C_2 are the integration constants, *cf.* Lecture 4.

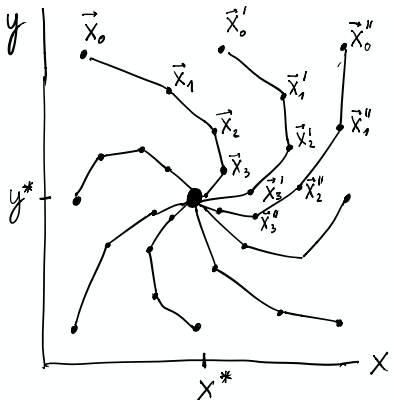

Figure 3: Phase portrait constructed from the initial conditions $\vec{x}_0$, $\vec{x}_0'$, $\vec{x}_0''$, etc. Trajectories suggest that the fixed point located at the origin $(x^*, y^*)^T = (0, 0)^T$ is a stable spiral.

Construction of a two-dimensional map phase portrait is analogues to the construction of phase portraits of continuous-time models given by (11), *cf.* Lectures 3 and 4. We select some number of uniformly distributed (or not) initial conditions and iterate them until the dynamics is revealed on the phase plane, see Fig. 3. In linear maps the fixed point satisfying $\vec{f}(\vec{x}^*) = \vec{x}^*$ is alway at the origin, i.e., $\vec{x}^* = \vec{0}$.

The following interactive numerical file calculates the iterates of linear maps and their phase portraits using the idea presented in Fig. 3.

NUMERICS: NB#2

Iterates of linear 2-D maps and their phase portraits.

1.5 Phase portrait of nonlinear 2-D map

Nonlinear phase portrait trajectories and actual map iterates that *should* hop along those trajectories may in fact not to do so and thus be confusing. This is especially true in chaotic maps that contain strange attractors. A more detailed and complete explanation is delayed until Secs 3.4 and 4.2.

2 Linearisation of 2-D maps

We know from our previous studies of continuous-time models that the type and stability of fixed points depends on eigenvalues of such systems. Maps are no different the type and stability of fixed point satisfying

$$\vec{f}(\vec{x}^*) = \vec{x}^*, \tag{13}$$

or in general of a period-p point satisfying

$$\vec{f}^p(\vec{x}) = \vec{x}, \tag{14}$$

where p denotes the map iterate, depends on the eigenanalysis of the system coefficient matrix which is defined by map function $\vec{f}$ in the case of linear $\vec{f}$, or on the eigenanalysis of the linearised map in the case of nonlinear $\vec{f}$.

Next, we focus on a nonlinear two-dimensional mapping and on its fixed points $\vec{x}^*$. The component form of map (5) in a two-dimensional setting is the following:

$$\begin{cases} x_{n+1} = f(x_n, y_n), \\ y_{n+1} = g(x_n, y_n), \end{cases} \tag{15}$$

where f and g are the given functions. The linearisation of the map implies the study of small deviations $\vec{w} = (k, l)^T$ where $|\vec{w}| \ll 1$ near the fixed point $\vec{x}^* = (x^*, y^*)^T$. The slightly perturbed iterate is given by

$$\vec{x}_n = \vec{x}^* + \vec{w}_n. \tag{16}$$

The map dynamics for the perturbed iterate is as follows

$$\vec{x}_{n+1} = \vec{f}(\vec{x}_n) = \vec{f}(\vec{x}^* + \vec{w}_n) = \begin{bmatrix} \text{Taylor series} \\ \text{about } \vec{x}^*, \\ \textit{cf.}\ \text{Lecture 5} \end{bmatrix} = \vec{f}(\vec{x}^*) + J\big|_{\vec{x}^*} \cdot \vec{w}_n + \underbrace{O(|\vec{w}_n|^2)}_{\text{h.o.t.}} \approx \underbrace{\vec{f}(\vec{x}^*)}_{=\vec{x}^*} + J\big|_{\vec{x}^*} \cdot \vec{w}_n, \tag{17}$$

$$\vec{x}_{n+1} \approx \vec{x}^* + J\big|_{\vec{x}^*} \cdot \vec{w}_n, \tag{18}$$

$$\underbrace{\vec{x}_{n+1} - \vec{x}^*}_{=\vec{w}_{n+1}} \approx J\big|_{\vec{x}^*} \cdot \vec{w}_n, \tag{19}$$

$$\vec{w}_{n+1} \approx J\big|_{\vec{x}^*} \cdot \vec{w}_n, \tag{20}$$

neglecting the higher order term (h.o.t.) $O(|\vec{w}_n|^2)$ yields the linearisation of the map about fixed point $\vec{x}^*$

$$\boxed{\vec{w}_{n+1} = J\big|_{\vec{x}^*} \cdot \vec{w}_n,} \tag{21}$$

where J is the Jacobian matrix of map (5) or (15) and it is given by

$$J = \begin{pmatrix} \dfrac{\partial f}{\partial x_n} & \dfrac{\partial f}{\partial y_n} \\ \dfrac{\partial g}{\partial x_n} & \dfrac{\partial g}{\partial y_n} \end{pmatrix}. \tag{22}$$

As mentioned above linearised map (21) has a fixed point at the origin $\vec{x}^* = \vec{0} = (0, 0)^T$ (for non-singular matrix $I - J|_{\vec{x}^*}$ where I is the identity matrix) just like in the continuous-time models. This is easy to confirm, since for $\vec{w} = \vec{0}$ we are positioned at the original fixed point $\vec{x}^*$ and perturbation $\vec{x}^* + \vec{0} = \vec{x}^*$.

3 Classification of fixed points in linear 2-D maps

The component form of the linearised map (21) is

$$\begin{pmatrix} k_{n+1} \\ l_{n+1} \end{pmatrix} = J\big|_{(x^*,y^*)^T} \cdot \begin{pmatrix} k_n \\ l_n \end{pmatrix} = \begin{pmatrix} a & b \\ c & d \end{pmatrix} \begin{pmatrix} k_n \\ l_n \end{pmatrix}, \tag{23}$$

where a, b, c, and d are the constant coefficients of the Jacobian matrix evaluated at the fixed point. The coefficients determine the eigenvalues and eigenvectors of map (21). Let's rename the coefficient matrix of the linearised map (23) to A, i.e.,

$$A = \begin{pmatrix} a & b \\ c & d \end{pmatrix}. \tag{24}$$

The following slides remind us how the eigenvalues and eigenvectors are related to the characteristic polynomial of coefficient matrix A.

SLIDES: 10, 11

2-D linear maps

Remainder from Lecture 4:

The (straight line) solution exists if one can find the λ's and $\vec{v}$'s. λ is given by

$$\det(A - \lambda I) = 0 \Rightarrow \begin{vmatrix} a-\lambda & b \\ c & d-\lambda \end{vmatrix} = \boxed{\lambda^2 - \tau\lambda + \Delta = 0}, \tag{3}$$

where the boxed part is called the characteristic equation of the system and where

$$\tau = a + d \quad \text{is the trace of matrix } A \tag{4}$$

and

$$\Delta = ad - bc \quad \text{is the determinant of matrix } A. \tag{5}$$

D. Kartofelev YFX1520 10 / 24

2-D linear maps

$$\boxed{\lambda^2 - \tau\lambda + \Delta = 0}$$

Algebraic form of λ is

$$\lambda_{1,2} = \frac{\tau \pm \sqrt{\tau^2 - 4\Delta}}{2}. \tag{6}$$

Additional *nice* propertied of λ and Δ are the following:

$$\tau = \lambda_1 + \lambda_2, \tag{7}$$

$$\Delta = \lambda_1 \lambda_2. \tag{8}$$

D. Kartofelev YFX1520 11 / 24

3.1 CASE I: Nodes and saddles

Criterion: Distinct real eigenvalues.

a) Stable node (sink) for $|\lambda_1|, |\lambda_2| < 1$.

Unstable node (source) for $|\lambda_1|, |\lambda_2| > 1$.

b) Saddle $|\lambda_1| \lesseqgtr 1 \lesseqgtr |\lambda_2|$. The classification graph, shown on Slide 12 and in Fig. 4, distinguishes two types of saddles: saddle sink, for $|\Delta| < 1$ where the area of linearly mapped region shrinks; and saddle source, for $|\Delta| > 1$ where the area grows.

3.2 CASE II: Degenerate nodes

Criterion: Repeated real eigenvalues $\lambda_1 = \lambda_2$.

a) A single uniquely determined eigenvector (the other one can be anything):

- Stable degenerate node (sink) for $|\lambda| < 1$, $|\Delta| < 1$.
- Unstable degenerate node (source) for $|\lambda| > 1$, $|\Delta| > 1$.

b) No uniquely determined eigenvectors (both can be anything, every direction is an eigendirection):

- Stable star (sink) for $|\lambda| < 1$, $|\Delta| < 1$.
- Unstable star (source) for $|\lambda| > 1$, $|\Delta| > 1$.

3.3 CASE III: Rotation

Criterion: Complex conjugate pair of eigenvalues $\lambda = \mu \pm \mathrm{i}\theta$. The general form of the coefficient matrix A is the following:

$$A = \begin{pmatrix} \cos\theta & -\sin\theta \\ \sin\theta & \cos\theta \end{pmatrix}, \tag{25}$$

where θ is the rotation angle per iteration.

a) Stable rotating spiral (sink or focus) for $|\lambda| = \sqrt{\mu^2 + \theta^2} < 1$, $|\Delta| < 1$.

Unstable rotating spiral (source or focus) for $|\lambda| = \sqrt{\mu^2 + \theta^2} > 1$, $|\Delta| > 1$.

b) The Lyapunov stable rotation (no change in area) for $|\lambda| = \sqrt{\mu^2 + \theta^2} = 1$, $|\Delta| = 1$. The Lyapunov stability implies that the iterates located close to the fixed point remain there for all time.

Note: In the above classification $|\Delta|$ is equal to the **change in area** of any initial condition (think: geometric shape) iterated (transformed) by the map per single iteration.

In the two-dimensional case the conditions for stability, i.e., for which $|\lambda_1|, |\lambda_2| < 1$, can be given a simple representation in terms of the trace τ and determinant Δ of the constant coefficient matrix A as follows

$$\begin{cases} 1 + \tau + \Delta > 0, \\ 1 - \tau + \Delta > 0, \\ 1 - \Delta > 0. \end{cases} \tag{26}$$

The dynamics for a linear map can be conveniently summarised by the diagram shown on Slide 12 and in Fig. 4. For simplicity's sake we represent phase portrait trajectories as continuous rather than dotted curves (marking the map iterate x_n). If we replace the greater-than sign with the equal sign in conditions (26), we obtain three lines intersecting in the $\Delta\tau$-plane, defining a triangle. The points inside the triangle correspond to **stable combinations** of τ and Δ of system matrix A. If $1 + \tau + \Delta = 0$ while (26)b and (26)c hold, one eigenvalue is equal to -1; if $1 - \tau + \Delta = 0$ while (26)a and (26)c hold, one eigenvalue is equal to $+1$; and if $\Delta = 1$ while (26)a and (26)b hold, the two eigenvalues are a complex conjugate pair with modulus equal to 1. The parabola defined by

$$\tau^2 - 4\Delta = 0, \tag{27}$$

shown with the red graph on Slide 12 and in Fig. 4 divides the $\Delta\tau$-plane into two regions corresponding to real eigenvalues (outside the parabola) and complex eigenvalues (inside the parabola) in the same manner as in the case of the continuous-time linear two-dimensional systems studied in Lecture 4. The **degenerate nodes** are found on the parabola (27). Combinations of τ and Δ inside the parabola but in the triangle lead to **stable spirals**, combinations outside the parabola but in the triangle are **stable nodes**. All other combinations lead to unstable fixed points—**saddles** and **nodes**.

SLIDE: 12

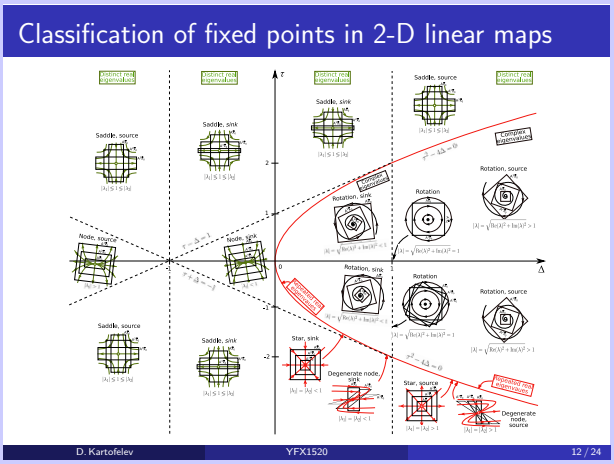

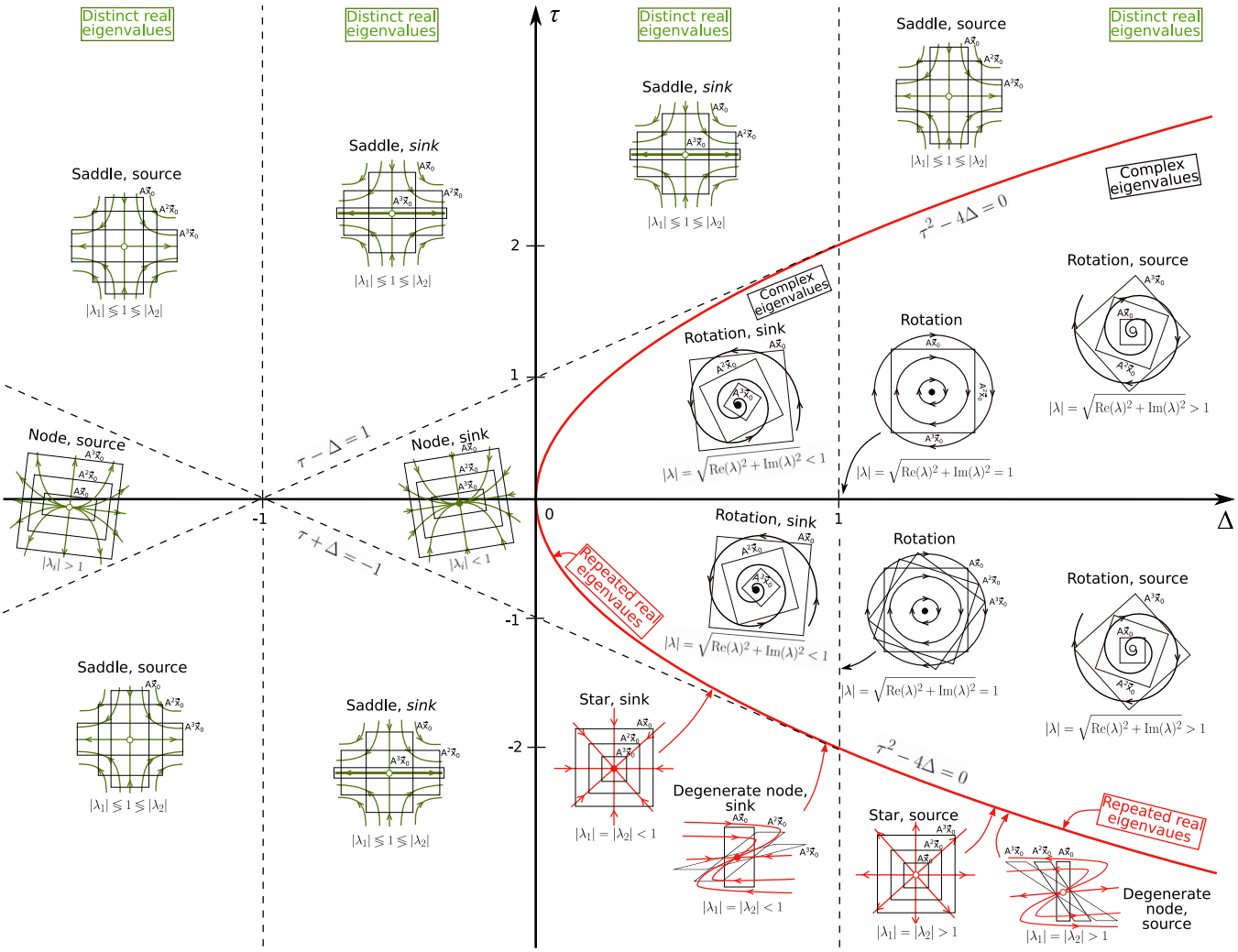

Figure 4: Classification of fixed points in linear two-dimensional maps where τ is the system matrix trace and Δ is the determinant of system matrix. Iterate *trajectories* are shown as continuous rather than dotted curves. Mapping of the rectangular regions is shown for three iterations. For $|\Delta| < 1$ the area of mapped rectangular regions shrinks (sink) and for $|\Delta| > 1$ the area grows (source).

The following numerical file presents interactive examples of all dynamics possible in linear two-dimensional maps. The maps are applied to a large number of points, i.e., initial conditions $\vec{x}_0$, that are placed randomly inside a rectangular region. This rectangular region is represented by the coloured rectangular outlines in the overview diagram shown on Slide 12 and in Fig. 4.

NUMERICS: NB#3

Examples of linear dynamics of 2-D maps. Classification of fixed points of linear maps: node, saddle, degenerate node, star, rotation.

3.4 Improper oscillation of iterates

At this point we ought to mention an important difference between solutions of continuous-time systems and solutions of discrete-time systems regarding the status of the invariant lines defined by the eigenvectors. The real eigenvectors associated with real eigenvalues for systems of recurrance equations (maps) are still invariant sets, i.e., sequences of points initiating on these sets remain on the sets. However the invariant, continuous, straight lines are not solution trajectories or orbits as they were in the continuous case, govern by solution in the form (12). Maps feature an interesting peculiarity **in the case of negative real eigenvalues** known as the **improper oscillations**. In such a case, we may have the following interesting situation. Consider again map (5). Suppose we have one real eigenvalue $\lambda_1 < 0$, $|\lambda_1| > 1$ and that

the initial condition $\vec{x}_0 = \vec{v}_1$ where $\vec{v}_1$ is the eigenvector corresponding to λ_1. Then according to (10) the solution is

$$\vec{x}_n = \lambda_1^n \vec{v}_1, \tag{28}$$

i.e., the system stays forever on the straight line through the origin defined by $\vec{v}_1$. At each iterate the system moves towards the fixed point $\vec{x}^* = \vec{0}$, but always overshoots it, so that the distance from $\vec{x}^*$ becomes ever larger with each iterate, tending to ∞ as $n \to +\infty$. This behaviour is shown in Fig. 5. Therefore, when there are negative real eigenvalues in discrete-time systems, great care should be applied in the use and, in particular, the interpretation of arrows in the phase portraits.

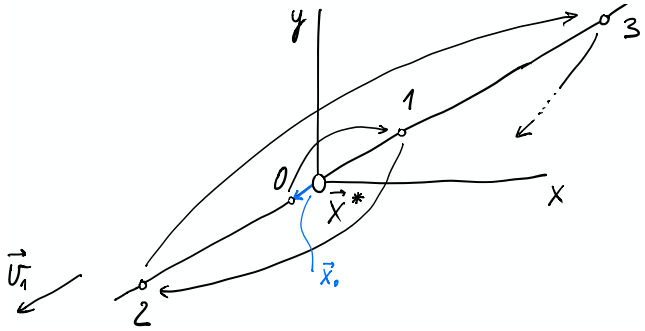

Figure 5: Improper oscillation of map iterates along the invariant line defined by the eigenvector $\vec{v}_1$ where $\lambda_1 < 0$, $|\lambda_1| > 1$.

On the other hand if $\lambda_1 < 0$ and $|\lambda_1| < 1$, then the iterates also oscillate improperly around the fixed point $\vec{x}^*$ but eventually approach it $\vec{x}_n \to \vec{x}^*$ as $n \to +\infty$, see Fig. 6. Slide 13 shows a more general case of the improper oscillations of iterates in the case of a stable node and a saddle.

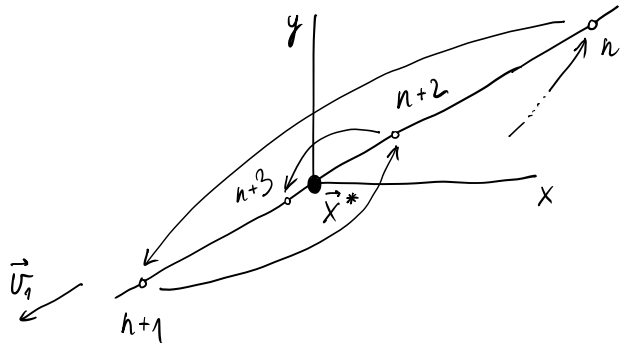

Figure 6: Improper oscillation of map iterates along the invariant line defined by the eigenvector $\vec{v}_1$ where $\lambda_1 < 0$ and $|\lambda_1| < 1$.

The following numerical file may be used to study the improperly oscillating iterates.

NUMERICS: NB#2

Iterates of linear 2-D maps and their phase portraits.

Example of improper oscillation in the stable node fixed point dynamics. Improper oscillation of iterates takes place, e.g., for the following system coefficient values: $a = 0.4$, $b = 0.1$, $c = 0.6$, $d = -0.5$.

The following slide shows improper oscillation taking place in a stable node and a saddle

SLIDE: 13

Classification of fixed points in 2-D linear maps

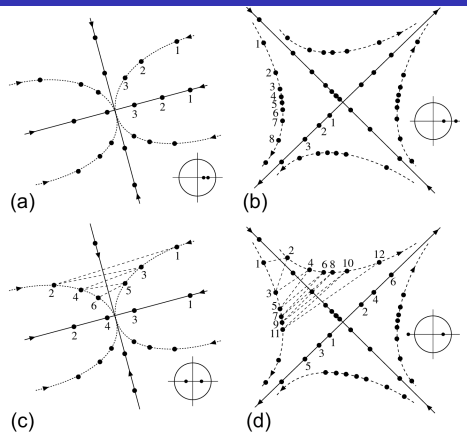

Figure: Phase portraits where the eigenvalues are distinct and real: (a) and (c) stable nodes, (b) and (d) saddles.

Negative eigenvalue forces the iterates to jump back and forth across the manifold (defined by the other eigendirection).

Image: A. Medio, M. Lines, *Nonlinear Dynamics: A Primer*, Cambridge University Press, 2001, p. 49

D. Kartofelev YFX1520 13 / 24

4 Linear analysis of the Hénon map

Now that we know how to perform linear analysis we apply it to our old friend the Hénon map.

4.1 Fixed points

SLIDES: 14, 15

Linear analysis of the Hénon map

The Hénon map[5] is defined by

$$\begin{cases} x_{n+1} = 1 + y_n - ax_n^2, \\ y_{n+1} = bx_n, \end{cases} \tag{9}$$

where a and b are the parameters.

[5] See Mathematica .nb file uploaded to the course webpage.

D. Kartofelev YFX1520 14 / 24

The Hénon map dynamics[6]

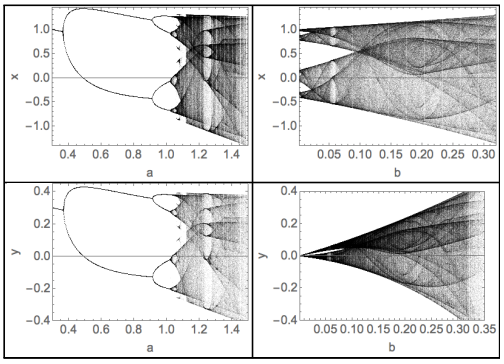

[6] See Mathematica .nb file uploaded to the course webpage.

D. Kartofelev YFX1520 15 / 24

Slide 15 shows the orbit diagrams of the chaotic Hénon map.

The Hénon attractor introduced in Lecture 12 and shown on Slide 14 is given by

$$\begin{cases} x_{n+1} = 1 + y_n - ax_n^2, \\ y_{n+1} = bx_n, \end{cases} \tag{29}$$

where a and b are the control parameters. A chaotic solution exists, e.g., for $a = 1.4$, $b = 0.3$. The map has **two fixed points** as was shown in Lecture 12. In two-dimensional maps the fixed points are defined the same way as in one-dimensional maps. The fixed point or period-1 point satisfies (13). In our case we use (29) and solve

$$\begin{cases} x^* = 1 + y^* - ax^{*2}, \\ y^* = bx^*, \end{cases} \tag{30}$$

for x^* and y^* to find the two fixed points $\vec{x}^*_\pm = (x^*_\pm, y^*_\pm)^T$ where

$$x^*_\pm = \frac{b-1 \pm \sqrt{4a+(b-1)^2}}{2a}, \qquad y^*_\pm = \frac{b\left(b-1 \pm \sqrt{4a+(b-1)^2}\right)}{2a}. \tag{31}$$

The higher period-p points also exist just like in one-dimensional maps. Period-p point satisfies (14). The numerical file linked below shows the above fixed points and also the period-2 point of the Hénon map.

NUMERICS: NB#4

The Hénon map dynamics: mapping and iterating a rectangle with the map; period-2 cycle trajectory in xy-plane; orbit diagram.

Same or very similar file was used during Lecture 12.

4.2 Linearisation

The linearisation of the Hénon map (29) and the linear analysis of the fixed points $\vec{x}_\pm$ defined by (31) is performed in the following numerical file.

NUMERICS: NB#5

Linear analysis of the Hénon map. Stability of its fixed points and their local dynamics.

The Hénon map (29) is evaluated using parameter values $a = 1.4$ and $b = 0.3$. The linearised map evaluated about the fixed point $\vec{x}^*_+$ given by (31) is

$$\vec{w}_{n+1} = \left.\begin{pmatrix} \frac{\partial x_{n+1}}{\partial x_n} & \frac{\partial x_{n+1}}{\partial y_n} \\ \frac{\partial y_{n+1}}{\partial x_n} & \frac{\partial y_{n+1}}{\partial y_n} \end{pmatrix}\right|_{\vec{x}^*_+} \cdot \vec{w} = \begin{pmatrix} 1-b-\sqrt{4a+(b-1)^2} & 1 \\ b & 0 \end{pmatrix} \vec{w} = \begin{pmatrix} -1.76779 & 1 \\ 0.3 & 0 \end{pmatrix} \vec{w}, \tag{32}$$

where the **real and distinct eigenvalues** are $\lambda_1 = -1.92374$ and $\lambda_2 = 0.155946$. The linearised map evaluated about fixed point $\vec{x}^*_-$ given by (31) is

$$\vec{w}_{n+1} = \left.\begin{pmatrix} \frac{\partial x_{n+1}}{\partial x_n} & \frac{\partial x_{n+1}}{\partial y_n} \\ \frac{\partial y_{n+1}}{\partial x_n} & \frac{\partial y_{n+1}}{\partial y_n} \end{pmatrix}\right|_{\vec{x}^*_-} \cdot \vec{w} = \begin{pmatrix} 1-b+\sqrt{4a+(b-1)^2} & 1 \\ b & 0 \end{pmatrix} \vec{w} = \begin{pmatrix} 3.16779 & 1 \\ 0.3 & 0 \end{pmatrix} \vec{w}, \tag{33}$$

where the **real and distinct eigenvalues** are $\lambda_1 = 3.25982$ and $\lambda_2 = -0.0920296$. In both cases it holds that $|\lambda_1| \lesseqgtr 1 \lesseqgtr |\lambda_2|$. According to Sec. 3.1 the type of fixed points $\vec{x}_\pm$ must be a **saddle**. Additionally, both cases feature improper oscillation of iterates, caused by the negative eigenvalues.

A visual inspection of the obtained results raises a justified question: Why is the full model (29) as a whole and locally near the fixed points $\vec{x}_\pm$ so different from the linearised maps (32) and (33)? In the case of the Hénon map and in other nonlinear maps in general the eigenvalues and eigenvectors are dependent on variables x and y (or k and l in linearised map notation). This means that a nonlinear map can be given in the form

$$\vec{x}_{n+1} = \begin{pmatrix} f_{1,1}(x_n, y_n) & f_{1,2}(x_n, y_n) \\ f_{2,1}(x_n, y_n) & f_{2,2}(x_n, y_n) \end{pmatrix} \vec{x}_n, \tag{34}$$

where the map matrix elements $f_{i,j}$ are the appropriately selected functions of x_n and y_n not constant coefficient values. This, in turn, means that the eigenvectors are not straight in the phase plane as is the case for linear maps. A linear map is given by

$$\vec{x}_{n+1} = \begin{pmatrix} a & b \\ c & d \end{pmatrix} \vec{x}_n, \tag{35}$$

where the corresponding coefficients are constant, see Fig. 7.

In addition to being non-straight the eigenvectors of nonlinear maps can also intersect each others complicating matters even further. This in fact happens in the Hénon map. Figure 8 shows an example of intersected eigenvectors. The intersection points of the eigenvectors are referred to as the **homoclinic mixing** points. The homoclinic mixing is directly connected to and responsible for the **stretching–folding–re-injection dynamics** in chaotic maps.

Figure 7: (Left) An example of non-straight eigenvectors $\vec{v}_1$ and $\vec{v}_2$ of a nonlinear map defined by (34). (Right) An example of eigenvectors $\vec{v}_1$ and $\vec{v}_2$ of a linear map defined by (35).

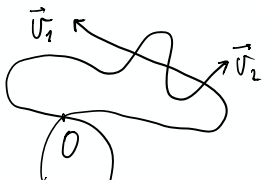

Figure 8: An example of intersected eigenvectors $\vec{v}_1$ and $\vec{v}_2$ of a nonlinear map defined by (34).

An in-depth discussion and analysis of the nonlinear maps and their phase portraits is omitted from this course. If you are interested in this topic one of our textbooks (K.T. Alligood, T.D. Sauer, J.A. Yorke, *Chaos: An Introduction to Dynamical Systems*, Springer, 2000) presents a good overview.

5 2-D discrete-time chaotic attractor

SLIDE: 16

Another example of a chaotic attractor existing in a map, alongside the Hénon map (29), is presented next. The following decoupled map is given in polar coordinates making its analysis more intuitive.

A chaotic map

Example[7]: A chaotic attractor in a 2-D map. The attractor is given in polar coordinates and in the following form:

$$\begin{aligned} r_{n+1} &= \sqrt{r_n}, \\ \theta_{n+1} &= 2\theta_n. \end{aligned} \tag{10}$$

[7] See Mathematica .nb file uploaded to the course webpage.

D. Kartofelev YFX1520 16 / 24

The following numerical file shown the dynamics of the chaotic attractor presented on Slide 16.

NUMERICS: NB#6

An example of discrete-time chaotic attractor: chaotic 2-D map given in polar coordinates.

Figure 9 shows the cobweb diagrams of the individual one-dimensional decoupled maps that form the two-dimensional map shown on Slide 16. In this example we see that SDIC of the linear map $\theta_{n+1} = 2\theta_n$ is contributing to the chaotic behaviour of the full two-dimensional dynamics.

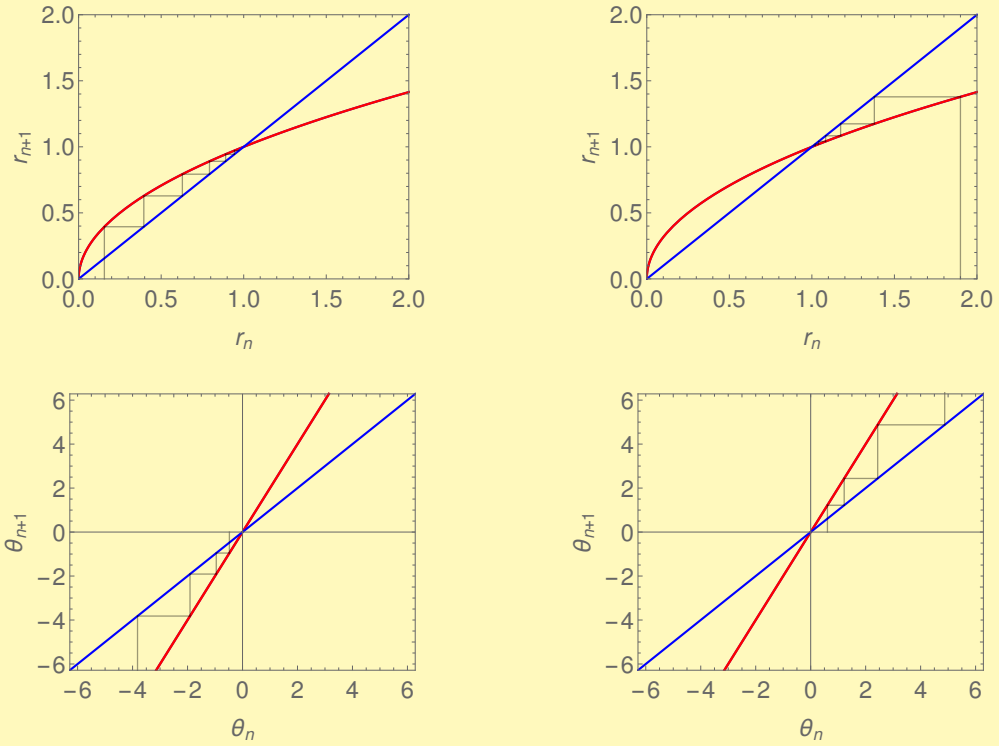

Figure 9: (Top row) Map dynamics in the radial direction shown for initial condition $r_0 < 1$ and $r_0 > 1$. (Bottom row) Map dynamics in terms of the angular displacement for initial angle $\theta_0 \lesssim 0$ and $\theta_0 \gtrsim 0$.

The analysis of the decoupled one-dimensional maps that form the full two-dimensional map leads us to conclude that the overall dynamics must be as shown in Fig. 10.

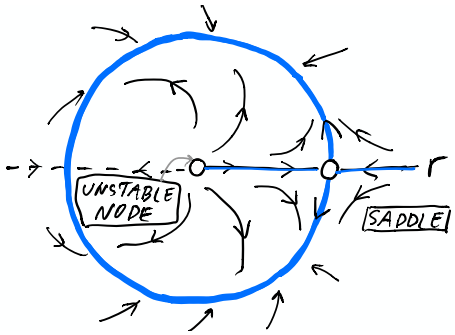

Figure 10: Phase portrait of the chaotic discrete-time attractor defined on Slide 16. Stable limit-cycle defined by the first equation is shown with the thick blue unit circle. The iterates of an initial condition *hop* along the phase portrait *trajectories*. Two invariant sets present in the phase portrait are indicated by the thin blue lines that are coinciding with the r-axis.

Numerical simulation of the map confirms the aforementioned conclusions.

NUMERICS: NB#6

An example of discrete-time chaotic attractor: chaotic 2-D map given in polar coordinates.

6 Video feedback effect

The nonlinear video feedback effect is a stunning visual example of a chaotic two-dimensional repeated mapping process—**a feedback loop**. The video feedback is the process that starts and continues when a video camera is pointed at its own playback video monitor. The loop delay from camera to display and back to camera prolongs for at least one video frame duration ($\approx 1/30$ s), due to the input and output scanning processes; it can be more if there is any additional video processing in the loop. As shown below this process can be understood as a 2-D nonlinear mapping problem that can lead to a chaotic solution.

SLIDES: 17–22

Video feedback effect

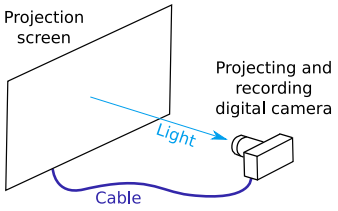

Figure: Basic setup for demonstrating the video feedback effect.

D. Kartofelev YFX1520 17 / 24

Video feedback effect

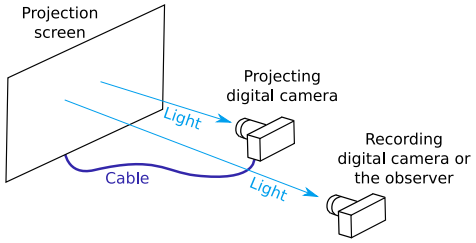

Figure: The setup in the following video.

D. Kartofelev YFX1520 18 / 24

Video feedback effect: 2-D mapping

Simplified (wrong) model of the effect.

$$\vec{F} \doteq \{c(x,y) \to c(f(x,y), g(x,y)\}, \tag{11}$$

or equivalently

$$c_{n+1}(x,y) = c_n(f(x,y), g(x,y)), \tag{12}$$

where continuous f and g are discretised:

$$\{x[i], y[j]\}, \text{ where } i,j \in \mathbb{Z},\ i \in [1,W],\ j \in [1,H]. \tag{13}$$

The projected image is composed of uniformly placed pixels $c[i,j]$. The total number of pixels is $W \cdot H$. n is the image frame number (iterate of the frame). Each pixel is assigned a colour depth value c (e.g. some 24 bit colour map, 8 bits per RGB channel totalling $2^{24} = 16\,777\,216$ colours). The functions f and g encompass all system dynamics and settings (camera, optics, electronics, digital signal processing, digital image transformations, etc.).

D. Kartofelev YFX1520 19 / 24

Video feedback effect: 2-D mapping

Alternative notation (more familiar to us). Component form:

$$\begin{cases} x^c_{n+1} = f(x^c_n, y^c_n) \\ y^c_{n+1} = g(x^c_n, y^c_n) \end{cases}, \quad \text{here} \quad x^c_n \in [1,W] \text{ and } y^c_n \in [1,H], \tag{14}$$

where each pixel (x,y) is assigned a colour c and each coordinate pair is sharing a colour, and n is the iterate (frame).

Matrix form:

$$\vec{c}_{n+1} = A\vec{c}_n, \qquad \vec{c} = \begin{pmatrix} x \\ y \end{pmatrix}, \tag{15}$$

where

$$A = \begin{pmatrix} a & b \\ c & d \end{pmatrix}, \quad \text{and } \{a,b,c,d\} \in \mathbb{R}, \tag{16}$$

or in the nonlinear case

$$A = \begin{pmatrix} f_{1,1}(x_n, y_n) & f_{1,2}(x_n, y_n) \\ f_{2,1}(x_n, y_n) & f_{2,2}(x_n, y_n) \end{pmatrix}, \quad f_{i,j} \text{ are the functions.} \tag{17}$$

D. Kartofelev YFX1520 20 / 24

Video feedback effect: video

No embedded video files in this pdf

D. Kartofelev YFX1520 21 / 24

Video feedback effect

What is/are the source/sources of the nonlinearity?
Hint: Compare to the optical feedback between mirrors.

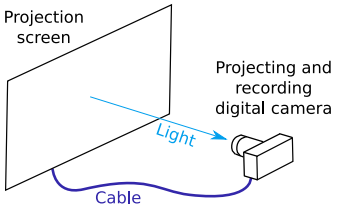

Figure: Basic setup for demonstrating the video feedback effect.

D. Kartofelev YFX1520 22 / 24

Discussion: The question posed on Slide 22 is discussed during the lecture in a group work exer-

cise setting. When answering the question keep in mind that the rotation and magnification are linear mappings (transformations), see Sec. 3.2 and Sec. 3.3. The hints that might be helpful in answering the question are given below.

Hints: Consider the following sources of nonlinearity: noise, optical aberration (arguably non-existent), digital image processing (stacked images), time-delay, nonlinear digital image interpolation over the discrete pixel grid/plane (under positive zoom and rotation), positive feedback. Consider comparing this effect to the optical feedback between two mirrors.

Revision questions

1. Is it possible to see stretching–folding–re-injection dynamics in cobweb plots?
2. What does linearisation of a nonlinear 2-D map imply?
3. Define sensitive dependence on initial conditions in maps.
4. Define basin of attraction of a map.
5. Sketch a saddle fixed point.
6. Sketch a stable node (sink) fixed point.
7. Sketch an unstable node (source) fixed point.
8. What are improper oscillations of map iterates?
9. What is the cause of improper oscillation of map iterates in terms of eigenvalues?
10. What is the video feedback effect?